Available online at www.sciencedirect.com

SciVerse ScienceDirect

Ceramics International 39 (2013) 1029–1036

CERAMICS INTERNATIONAL

www.elsevier.com/locate/ceramint

Luminescent properties of Gd^{3+} sensitized low-phonon energy $CaGd_4O_7:Tb^{3+}$ green emitting novel phosphors

E. Pavitra, Jae Su Yu*

Department of Electronics and Radio Engineering, Institute for Laser Engineering, Kyung Hee University, 1 Seocheon-dong, Giheung-gu, Yongin-si, Gyeonggi-do 446-701, Republic of Korea

Received 22 June 2012; received in revised form 4 July 2012; accepted 4 July 2012
Available online 14 July 2012

Abstract

The trivalent terbium (Tb^{3+}) ions activated $CaGd_4O_7$ (CG) phosphors were synthesized by a sol–gel method. The characterizations were performed after the samples annealed at 1500 °C. The structural and morphological properties were analyzed from the X-ray diffraction patterns and scanning electron microscope images. The photoluminescence excitation spectra showed a broad-band between the wavelengths 250 and 300 nm, which were overlapped with the Gd^{3+} excitation bands. The photoluminescence spectra exhibited efficient green emission due to the sensitization effect of Gd^{3+} ions on the Tb^{3+} ions when exciting with the Gd^{3+} wavelength at 278 nm. In order to analyze the influence of Tb^{3+} concentration on the luminescence behavior of Tb^{3+} ions in the CG host lattice, the decay curves were measured. The temperature-dependent luminescence measurements were done to identify the thermal stability of CG:Tb^{3+} phosphors at elevated temperatures. The cathodoluminescent spectra also showed a similar behavior to that observed in PL spectra. The CIE chromaticity coordinates as a function of Tb^{3+} concentration were calculated and all the obtained chromaticity coordinates have been placed in the green spectral region.

Keywords: A. Sol–gel processes; $CaGd_4O_7$; Luminescence properties; Lifetime analysis

1. Introduction

The trivalent rare-earth (RE^{3+}) ions doped oxide phosphors, which may possibly become promising materials for optoelectronic devices and flat-panel display systems [1–3], have attracted a great attention in order to replace the traditional sulfide phosphors owing to their chemical, mechanical, and thermal stability. It is well known that the RE ions are famous because of their extremely rich $4f^N$ ($N=1$–14, from Ce^{3+} to Yb^{3+}) electronic energy configurations [4]. Several transitions are available between the $4f^N$ states in the visible region, and these transitions are almost insensitive to the local environment because 4f orbitals are shielded by the completely filled 5s and 5p electronic subshells [1,5]. This perception indicates that these active RE ions are not necessarily located in a specific crystal lattice position, as in the case of 4f–5d transitions. However, it is easy to find out the occupation of sites in the host lattice if certain RE^{3+} ions such as (Eu^{3+}, Dy^{3+} and Sm^{3+}) are located in the specified lattice [6,7]. This is an obvious advantage for the development of new types of phosphors, which may decrease the fabrication cost as well. Among these RE^{3+} ions, it is well known that the Tb^{3+} ions emit blue emission at lower concentration and green emission at higher concentration. However, the emission of light not only depending upon the concentration of Tb^{3+} ions but also depending upon the phonon energies of the host lattice [8].

The rapidly expanding market for solid-state lighting creates a need for the development of novel phosphors with high conversion efficiencies, excellent thermal quenching behavior and the efficient emissions in the visible spectral range. Unlike incandescent and fluorescent lamps, LEDs are not characteristically white light sources. LEDs emit light in a very narrow range of wavelengths in the visible spectrum, resulting in nearly monochromatic light. Thus, LEDs are so efficient for colored light applications

*Corresponding author. Tel.: +82 31 201 3820; fax: +82 31 206 2820.
E-mail address: jsyu@khu.ac.kr (J. Su Yu).

0272-8842/$36.00
http://dx.doi.org/10.1016/j.ceramint.2012.07.023

such as traffic lights and exit signs. At present, mainly two ways to make White light-emitting diodes (WLEDs) i.e., blue LED chip coated with yellow phosphor and the tri-band (Red, Green, and Blue) based WLEDs, which have been fabricated by pumping the UV-A (320–400 nm) LED sources. The tri-band based WLEDs offer good color flexibility both in multicolor displays and different shades of white and also excellent color rendering index [9].

Generally, phosphors are prepared by a traditional solid-state reaction method [10]. This approach naturally requires high temperature, time-consuming heating process and subsequent grinding [3,7,11–13]. The grinding process damages the phosphor surfaces, causing the loss of emission intensity. Additionally, phosphor particles prepared through this solid-state reaction method are large in size (generally in micrometer range). However, in recent years, several wet chemical techniques such as the co-precipitation method [14], combustion [15], hydrothermal [6], solvothermal [2], spray-pyrolysis [16], and sol–gel [17] were employed to prepare the phosphor precursor. Among these techniques, the sol–gel process has attracted much attention because of its advantages for obtaining the novel chemical compositions with unique properties, excellent purity and relatively low reaction temperature resulting in more homogeneous products, and it is also possible to synthesize phosphors with small sizes [18].

To the best of our knowledge, so far no reports have been found on the luminescent properties of $CaGd_4O_7$ (CG) host lattice based phosphors. In this work, we reported on the synthesis of Tb^{3+} activated monoclinic CG host lattice by means of a sol–gel process, together with the detailed analysis of X-ray diffraction (XRD) patterns, scanning electron microscope (SEM), photoluminescence (PL) along with decay curves, temperature-dependent luminescence and cathodoluminescence (CL) properties.

2. Experimental

The $CaGd_4O_7$ nanocrystalline phosphors with different concentrations of Tb^{3+} were prepared by means of the sol–gel method by taking the stoichiometric amounts of high-purity grade calcium nitrate hexahydrate [$Ca(NO_3)_2 \cdot 4H_2O$], gadolinium nitrate hexahydrate [$Gd(NO_3)_3 \cdot 6H_2O$], terbium nitrate pentahydrate [$Tb(NO_3)_3 \cdot 5H_2O$] and citric acid [$HOC(COOH)(CH_2COOH)_2$]. One solution was prepared by dissolving the 1 mM of calcium nitrate, 2 mM of citric acid in de-ionized (DI) water. The other solution was prepared by dissolving the $4(1-x)$ mM of gadolinium nitrate, $4x$ mM of terbium nitrate and 8 mM of citric acid in DI water. The two solutions were stirred individually by the magnetic stirrer for 30 min, and then they were mixed and stirred until a homogeneous solution was formed. The mixture was then heated on a hot plate with continued magnetic stirring, and the solution temperature was maintained at 80 °C. Firstly, the beaker was closed with a cap for 12 h and then the cap was removed. After opening the cap, the solution was evaporated within 1 h and yellowish wet gel was produced. The gel was dried at 120 °C, which yields porous solid matrices called xerogel. The drying was accompanied by liquid expulsion from the pores (syneresis) and substantial matrix shrinkage often leads to cracks (mainly due to the capillary pressure). This precursor decomposed to give black-colored flakes with extremely fine particle size by further calcination at 400 °C for 4 h. The resulting sample was further annealed at 1500 °C for 10 h. But Tb doped phosphors showed no emission after annealing treatment in the ambient atmosphere, which indicates that all the Tb ions are in the tetravalent state. To convert Tb^{4+} to Tb^{3+} for obtaining emission properties, all the heat treatment powders were then fired under a reduced atmosphere (4% H_2/96% Ar) at 1400 °C for 3 h, and the powders body color changes from yellow to white. This indicates that all terbium ions are in the trivalent state.

3. Results and discussion

Fig. 1 shows the XRD pattern of $CaGd_4O_7$ (CG) powder phosphor sample, which was annealed at 1500 °C for 10 h. At this temperature the CG phosphor was well crystallized into monoclinic phase with the space group B2/m. The calculated lattice constants are $a=22.43$, $b=8.81$, and $c=3.73$, which were very close to the standard JCPDS card [PDF (72-2492)]. Typically, the crystallite size can be estimated by using the Scherrer equation, $D_{hkl}=k\lambda/(\beta \cos\theta)$, where D is the average grain size, k (0.9) is a shape factor, λ is the X-ray wavelength (1.5406 Å), β is the full width at half maximum (FWHM) and θ is the diffraction angle of an observed peak. The strongest diffraction peaks are used to calculate the crystallite size, which yield an average value of about 98.4 nm. The inset of Fig. 1 shows the SEM image of the CG:Eu^{3+} phosphors annealed at 1500 °C. The closely

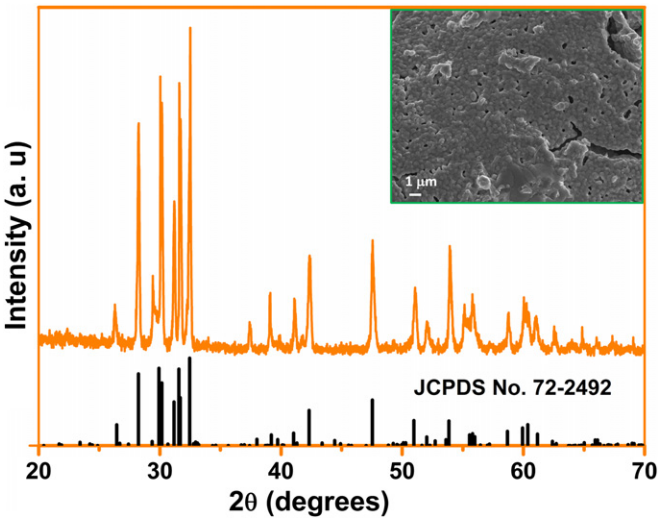

Fig. 1. XRD pattern of CG:2 mol% Tb^{3+} phosphor and the inset shows the corresponding SEM image.

packed particles were observed, which prevent the scattering of light, and yield the efficient light output.

Fig. 2 shows the photoluminescence excitation (PLE) spectra of the CG:Tb^{3+} phosphors as a function of Tb^{3+} concentration by monitoring the emission wavelength at 544 nm. The PLE spectra exhibited the broad band from 250 to 325 nm with band maxima at about 286 nm due to f–d transition of Tb^{3+}, and in the longer wavelength region, weaker f–f transitions of the Tb^{3+} ions due to $^7F_6 \rightarrow {}^5D_3$ and $^7F_6 \rightarrow {}^5D_4$ transitions were observed.

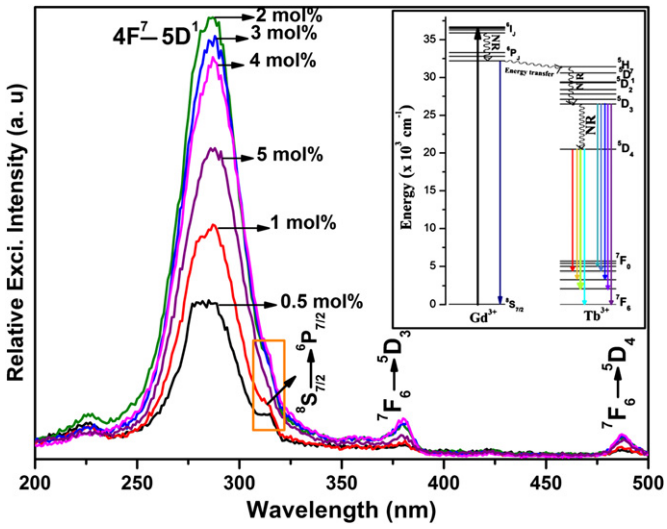

Fig. 2. PLE spectra of CG:Tb^{3+} phosphor as a function of Tb^{3+} concentration. The inset shows the energy transfer mechanism between Gd^{3+} and Tb^{3+} ions.

Usually, several f–f transitions of the Gd^{3+} ions are observed in the wavelength range 250–316 nm from the $^8S_{7/2}$ ground state to the excited levels (^6D_J, ^6I_J, ^6P_J) [19]. However, in the present work, only week $^8S_{7/2} \rightarrow {}^6P_{7/2}$ transition was observed at the lower Tb^{3+} concentration and was also disappeared when increasing the Tb^{3+} concentration, which indicates that the efficient energy transfer occurred from Gd^{3+} to Tb^{3+} ions. The energy transfer mechanism was presented in the inset of Fig. 2. It is noticeable that, when the Tb^{3+} concentration increases from 2 to 5 mol%, the f–d transition slightly moves towards the lower energy side from 286 to 288 nm. The reason is that the crystal-field splitting increases with increasing the Tb^{3+} concentration due to the shortening of distance between the central metal (Gd) ion and its ligands (O). Therefore, the energy level separation increases, which change the position of f–d transition.

Fig. 3 shows the photoluminescence (PL) spectra of the CG:Tb^{3+} phosphor as a function of Tb^{3+} concentration by exciting at 278 nm. The weak emission peak at 316 nm in the UV region is related to the 4f–4f intra-configurational $^6P_{7/2} \rightarrow {}^8S_{7/2}$ forbidden transition of Gd^{3+} ions, and all the remaining peaks belong to the typical emission of Tb^{3+} ions. At lower concentrations, Tb^{3+} ions show two groups of emission transitions in the visible region. One group of emission bands located at 380 ($^5D_3 \rightarrow {}^7F_6$), 415 ($^5D_3 \rightarrow {}^7F_5$), 438 ($^5D_3 \rightarrow {}^7F_4$), and 469 ($^5D_3 \rightarrow {}^7F_2$) nm. While, the other group of emission bands holding at 489, 544, 588 and 622 nm belong to the $^5D_4 \rightarrow {}^7F_J$ (J=6, 5, 4 and 3) transitions [20]. However, the position of terbium ions is hardly influenced due to the screen effect of 4f electrons

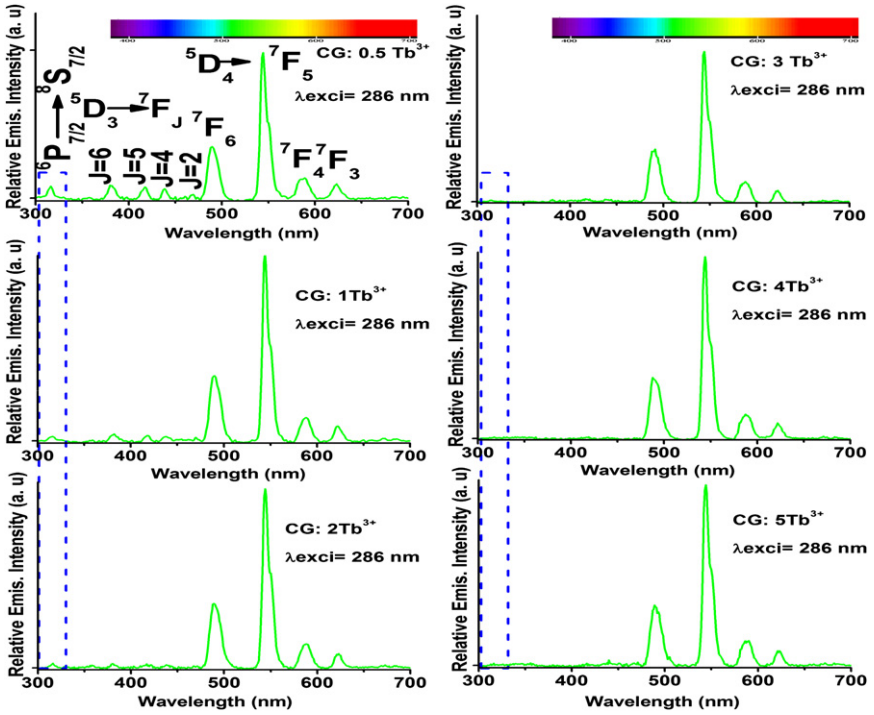

Fig. 3. PL spectra of CG:Tb^{3+} phosphor as a function of Tb^{3+} concentration. The dotted lines shows the Gd^{3+} emission intensity variation. (For interpretation of the references to color in this figure, the reader is referred to the web version of this article.)

protected by its outer electron layer. It is well known that, at dilute concentration, Tb^{3+} ions show strong emission bands in both blue and green regions, but increasing the Tb^{3+} concentration the emission peak intensities in the blue region have been suppressed due to the cross-relaxation effect. In the present work, the $^5D_3$ emissions are very weak as compared to the other host materials because the $^5D_3$ emission is related to both Tb^{3+} concentration and the phonon energies of the host lattice [2,21,22]. If the host lattice has greater phonon energies, the $^5D_3$ emission intensity becomes greater at diluted concentrations, while the phonon energies are small and the $^5D_3$ emission intensities are also small. From the observed results, we thought that the phonon energies of CG are relatively small. The main peak due to magnetic dipole transition $^5D_4 \rightarrow {}^7F_5$ holding at 544 nm in the pure green region can be explained by the large values of the reduced matrix element at $J=5$ and the Judd–Ofelt theory [23,24].

It is the noticeable fact that the intensity of the emission from the $^5D_4$ energy levels of Tb^{3+} ions increases with increasing the Tb^{3+} concentration and UV emission of Gd^{3+} ions at 316 nm ($^6P_{7/2} \rightarrow {}^8S_{7/2}$) decreases, in agreement with the increase in the energy transfer between Gd^{3+} and Tb^{3+}, as shown in dotted lines of Fig. 3. The corresponding emission intensity comparison of Gd^{3+} and Tb^{3+} ions are also illustrated in Fig. 4(a). The energy transfer probability from Gd^{3+} to Tb^{3+} is related to the concentration of Tb^{3+} ions. If the concentration of Tb^{3+} increases, the distance between Gd^{3+} and Tb^{3+} ions decreases and it acquires higher energy transfer efficiency. So the Gd^{3+} emission intensity decreases dramatically and the enhancement in Tb^{3+} emission intensity occurs. Usually, at room temperature, almost prominent energy transfer occurs from Gd^{3+} to Tb^{3+} because the $^6P_{7/2}$ level of Gd^{3+} is about 660 cm^{-1} higher than that of the $^5H_7$ level of Tb^{3+}, and the probability of emitting phonons for the Gd^{3+} ($^6P_{7/2}$) $\rightarrow Tb^{3+}$ ($^5I_7$) process is much higher than that of capturing phonons for the inverse process, as can be seen in the set of Fig. 2. Thus, the phonons assisted energy transfer enhances the population of Tb^{3+} ($^5D_3$) and ($^5D_4$) levels, resulting in the sensitization of the luminescence.

Figs. 3 and 4(a) also shows the concentration effect on the luminescence properties of Tb^{3+} activated CG phosphors by exciting with the wavelength of 278 nm. From Fig. 3, it is clear that, the intensity of the blue emission from $^5D_3$ levels decreases with increasing the Tb^{3+} concentration due to the cross-relaxation, and almost disappears at higher concentrations because of the closer energy differences between the $^5D_3$ and $^5D_4$ (5600 cm^{-1}) and the $^7F_0$ and $^7F_6$ (5800 cm^{-1}) levels. If two Tb^{3+} ions are closer to each other, a resonance condition can exist where the conversion of an electron from the $^5D_3$ to $^5D_4$ state was matched by the promotion of an electron from the $^7F_6$ to $^7F_0$ state. The electron fell down from the $^7F_0$ level to the $^7F_6$ ground state by the non-radiative process, and the energy was dissipated possibly by phonons. This process would cause the $^5D_4$ level to be fed from the $^5D_3$ level at a faster rate than that occurring in the case of a lone terbium ion, where the rate is depending upon the spontaneous decay rate of the $^5D_3$ state. The cross-relaxation process between the excited Tb^{3+} (donor) in $^5D_3$ state and second Tb^{3+} (acceptor) in the ground-state [25–27], which has been shown in Fig. 4(b). It can also be found that the $^5D_4 \rightarrow {}^7F_2$ emission intensity increases up to 2 mol% of Tb^{3+} ions in the CG host lattice and above that concentration, the emission intensity was decreased due to concentration quenching, as can be seen in Fig. 4(a). The concentration quenching mechanism can be elucidated by the following two factors: (i) when the doping concentration increases, the excitation migration becomes higher owing to the resonance between the activators, and thus the excitation energy reaches quenching centers, and (ii) the activators are combined or coagulated and are transformed to quenching center [7]. However, the samples up to 5 mol% of Tb^{3+} concentration were explored for observing the disappearance of $^5D_3$ emission intensity.

In order to analyze the influence of Tb^{3+} ions on the luminescence behavior of Tb^{3+} activated CG phosphors the decay curves were measured. The decay curves of the $^5D_4$

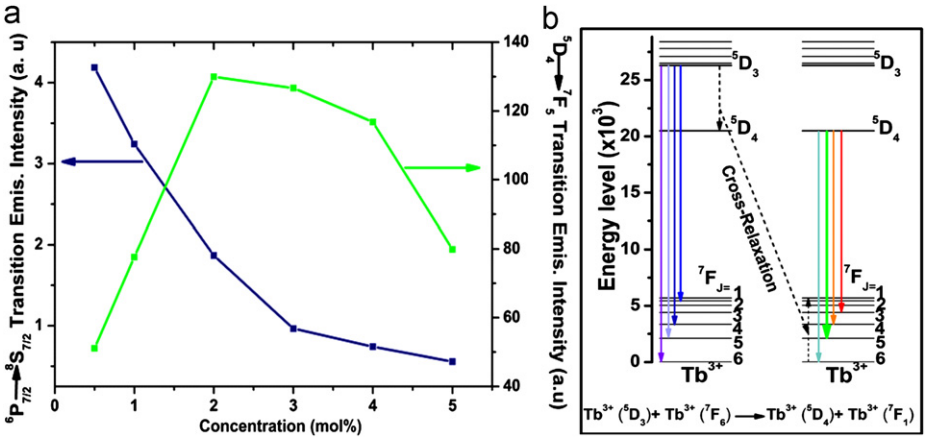

Fig. 4. **(a)** Gd^{3+} ($^6P_{7/2}$) and Tb^{3+} ($^5D_4$) emission intensity comparison as a function of Tb^{3+} concentration, and (b) the cross-relaxation process between Tb^{3+} ions. The equation of (b) shows the mechanism of the cross-relaxation process.

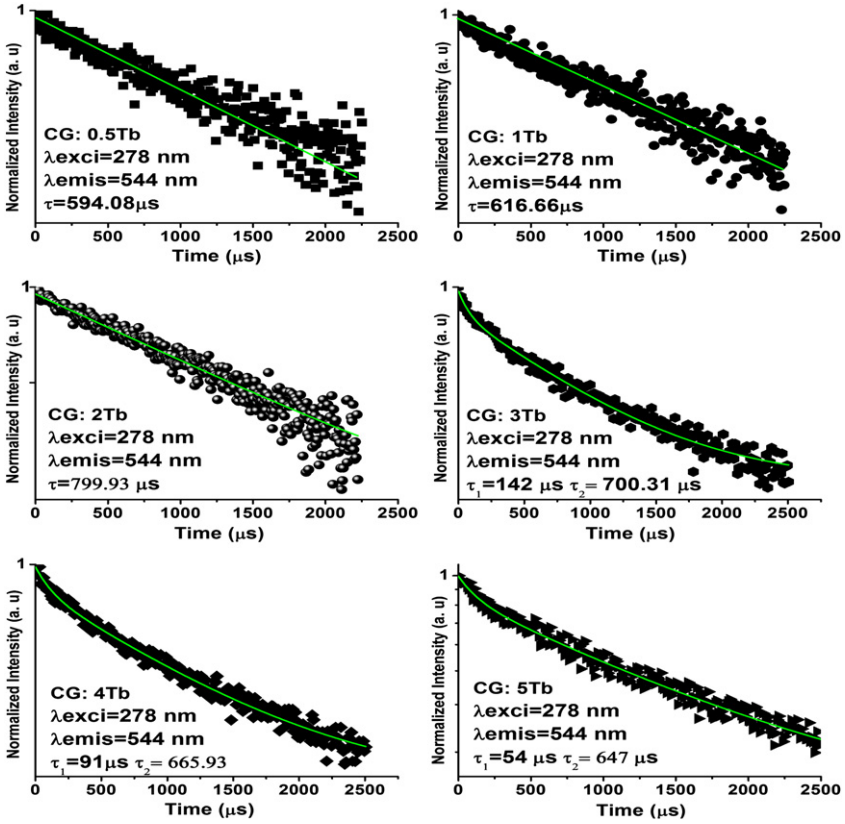

Fig. 5. Decay curves of CG:Tb^{3+} phosphor as a function of Tb^{3+} concentration.

level of CG:Tb^{3+} phosphors as a function of Tb^{3+} concentration were recorded under the excitation at 278 nm and the emission at 544 nm ($^5D_4 \rightarrow {}^7F_5$) was shown in Fig. 5. Up to 2 mol% of Tb^{3+} ions doped in CG host lattice, the decay curves were well fitted by a single exponential function, and above 2 mol% the decay curves were fitted to bi-exponential function. When the concentration increased to 2 mol% the lifetime increases from 594.08 to 799.93 μs. with a further increase of concentration, the non-exponential decay curves were observed and the long-life time (τ_2) value decreases, which is well correlated with the emission analysis. The increased cross-relaxation between $^5D_3$ and $^5D_4$ levels or the increased energy transfer efficiency between Gd^{3+} and Tb^{3+} ions are probably responsible for the non-exponential part at the initial level of the decay curve [10,11].

Owing to the importance of thermal quenching property in the technological parameters, the temperature-dependent luminescence properties of phosphors were measured for examing the suitability of their applications in the development of WLEDs [28,29]. The thermal quenching temperature, T_{50}, is defined as the temperature at which the emission intensity is 50% of its original value. Generally, it is necessary to keep the junction temperature of LEDs below 120 °C to run the LEDs for a maximum lifetime [30]. So high temperature ($\geq$120 °C) thermal quenching phosphor is the basic requirement for the fabrication of phosphor based LEDs. Thus, we performed the temperature-dependent measurements in the temperature range of 25–200 °C for the CG: 2 mol% Tb^{3+} phosphor. Fig. 6(a) shows the temperature dependent luminescence spectra of the CG:Tb^{3+} phosphors by exciting at 278 nm with the intervals of 5 °C from 25 to 200 °C. The inset of Fig. 6(a) shows the corresponding emission peak intensity as a function of temperature. Clearly, the emission intensity decreases linearly with increasing the temperature due to the thermal quenching. The emission intensity droped drastically by ~70% of its original intensity at 200 °C, and the shift of emission peak was not observed. It is well known that the trivalent terbium ions containing phosphors are heating in the ambient atmosphere and then the Tb^{3+} ions are easily converting to Tb^{4+} ions. It is known that the Tb^{4+} ions have no emission, so by increasing the temperature the emission intensity was decreased rapidly. However, CG:Tb^{3+} phosphors are suitable for UV-LEDs because the thermal quenching of CG:Tb^{3+} sample was observed at 140 °C. The average chromaticity coordinates were placed in the green region (0.331, 0.521), which are suitable for the generation of triband based white light emission [31].

In order to estimate the thermal activation energy of the novel green emission, the temperature-dependence of the normalized emission intensity was fitted with the well-known Arrhenius equation: [32–34]

$$I_{(T)} \approx \frac{I_{(0)}}{1 + c\exp(-\frac{\Delta E}{kT})}$$

Where $I_{(0)}$ is the initial intensity, $I_{(T)}$ is the intensity at the given temperature T, c is constant, k is the Boltzmann's constant, which was taken in eV, and ΔE is the activation energy for thermal quenching. According to the Arrhenius equation, the plot was drawn between $\ln[I_{(0)}/I_{(T)}-1]$ Versus $1/(kT)$ and used the linear fitting for observing the activation energy, as shown in the Fig. 6(b). From Fig. 6(b) and according to Arrhenius equation, the activation energy was found to be 0.22 eV, which signifies the good thermal stability of CG:Tb^{3+} green phosphor.

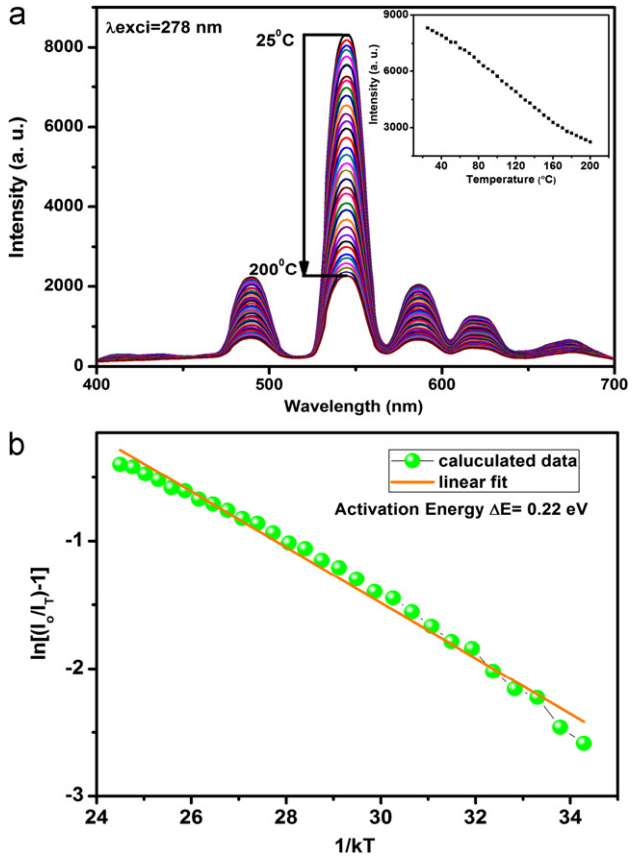

Fig. 6. (a) Temperature dependent luminescent properties of CG: 2 mol% Tb^{3+} phosphor as a function temperature, and (b) Activation energy of thermal quenching of CG: 2 mol% Tb^{3+} green phosphors fitted with Arrhenius equation.

Fig. 7(a) shows the CL spectra of 2 and 4 mol% Tb^{3+} activated CG phosphor at a constant accelerating voltage (5 kV) and a filament current (60 μA). The shape of the CL spectra is the same as PL except the intensity. However, the difference from PL is that the 2 mol% Tb^{3+} doped CG phosphor exhibits very weak $^5D_3$ emissions of Tb^{3+} and $^6P_{7/2}\rightarrow{}^8S_{7/2}$ transition of Gd^{3+} in PL spectrum whereas the $^5D_3$ emissions including Gd^{3+} emission intensities are somewhat strong in CL as compared to PL, and which were almost disappeared at 4 mol% of Tb^{3+} doped CG phosphor. The reason is that the CL mechanism is different from PL one. In PL, the phosphors are excited by photons of UV or visible light with the energy of only 4–6 eV, while for CL, the energy of fast electrons under the acceleration of anode voltage can be tuned from a thousands of electron volts. Thus, the excitation energy on individual ion is much larger in CL than that in PL. Therefore, in CL, the energy transfer and cross-relaxation process occurs at relatively higher concentrations than that in PL [35,36].

Fig. 7(b) and (c) shows the CL intensities as a function of accelerating voltage and filament current. From Fig. 7(b), clearly, when the filament current was fixed at 55 μA, the CL intensity of the phosphor increased with increasing the accelerating voltage from 1 to 5 kV and no optimization was observed up to 5 kV. The CL intensity increased with increasing the filament current from 35 to 55 μA under a fixed accelerating voltage of 5 kV as shown in Fig. 7(c). The reason is that the more plasma will be produced when increasing the filament current or accelerating voltage due to the deeper electron penetration depth by the recombination of more electron–hole (excitons) pairs, resulting in more Tb^{3+} ions from the

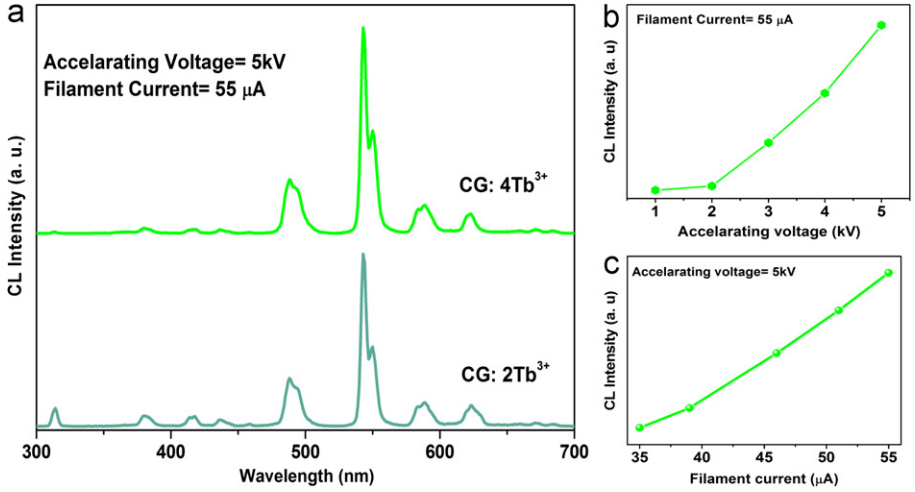

Fig. 7. (a) CL spectra of CG:Tb^{3+} (2 and 4 mol%) phosphors (b) CL emission intensity comparison for CG: 2Tb^{3+} as a function of accelerating voltage, and (c) CL emission intensity comparison for CG: 2Tb^{3+} as a function of filament current.

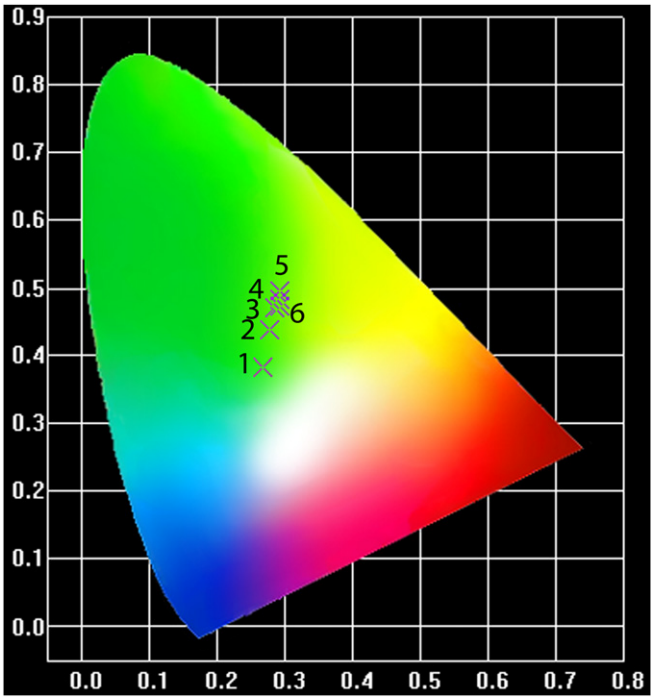

Fig. 8. Calculated CIE chromaticity coordinates of CG:Tb^{3+} phosphor as function of Tb^{3+} concentration [(1) 0.5 mol%, (2) 1 mol%, (3) 2 mol%, (4) 3 mol%, (5) 4 mol%, and (5) 5 mol% of Tb^{3+} ions in CG host lattice]. (For interpretation of the references to color in this figure, the reader is referred to the web version of this article.)

boundary or surface including the inside of the particles being excited [36]. The behavior of increased intensity with increasing the accelerating voltage and filament current of phosphors is useful for their application in FED systems.

Commission International De I-Eclairage (CIE) chromaticity coordinates of CG:Tb^{3+} phosphors as a function of Tb^{3+} concentration were calculated and represented in Fig. 8. The calculated CIE chromaticity coordinates are (0.268, 0.382), (0.277, 0.438), (0.286, 0.470), (0.292, 0.483), (0.293, 0.494), and (0.292, 0.472). From the observed results, it is evident that the green color purity increases because the emission intensity decrease in the blue region due to increased cross-relaxation between the Tb^{3+} ions with increasing the Tb^{3+} concentration. These coordinates are close proximities with the commercial green phosphor ZnS:Cu, Al (0.284, 0.605) [37], and Zn_2SiO_4:Tb^{3+} (0.287, 0.554) [38].

4. Conclusion

We have successfully prepared the CG:Tb^{3+} phosphor by means of the sol–gel process. The XRD patterns confirmed their monoclinic structure. The PLE spectra showed broad-band excitation in the UV region due to the 4f–5d transition of Tb^{3+} ions, and it was overlapped with the Gd^{3+} f–f transition. The PL spectra exhibited the excellent green emission due to the efficient energy transfer from Gd^{3+} to Tb^{3+} ions, and the observed chromaticity coordinates were in close proximity to the commercially available green phosphor coordinates. The optimized concentration of Tb^{3+} was found to be 2 mol%, but the green color purity was increased with increasing the Tb^{3+} concentration due to the cross-relaxation between the Tb^{3+} ions. The temperature-dependent luminescent properties indicate that this phosphor is suitable for the development of the tri-band based WLEDs because the thermal quenching was observed at 140 °C, and the activation energy was found to be 0.22 eV. The CL spectra showed the CL emission intensity potentiality as a function of accelerating voltage and filament current. These results provide a promising application possibility of these phosphors in the green region to produce white-light for UV-LEDs as well as optical display systems.

Acknowledgments

This work was supported by Basic Science Research Program through the National Research Foundation of Korea (NRF) funded by the Ministry of Education, Science and Technology (no. 2011-0026393).

References

[1] S.-A. Yan, J.-W. Wang, Y.-S. Chang, W.-S. Hwang, Y.-H. Chang, Synthesis and photoluminescence properties of $Ba_{1-y}Sr_yLa_{4-x}Dy_x(WO_4)_7$ (x=0.04–0.2, y=0–0.4) phosphors, Ceramics International 38 (3) (2012) 2569–2574.

[2] G.S.R. Raju, J.Y. Park, H.C. Jung, E. Pavitra, B.K. Moon, J.H. Jeong, J.H. Kim, Excitation induced efficient luminescent properties of nanocrystalline Tb^{3+}/Sm^{3+}:$Ca_2Gd_8Si_6O_{26}$ phosphors, Journal of Materials Chemistry 21 (17) (2011) 6136–6139.

[3] G. Li, D. Geng, M. Shang, C. Peng, Z. Cheng, J. Lin, Tunable luminescence of Ce^{3+}/Mn^{2+}-coactivated $Ca_2Gd_8(SiO_4)_6O_2$ through energy transfer and modulation of excitation: potential single-phase white/yellow-emitting phosphors, Journal of Materials Chemistry 21 (35) (2011) 13334–13344.

[4] W.T. Carnall, G.L. Goodman, K. Rajnak, R.S. Rana, A systematic analysis of the spectra of the lanthanides doped into single crystal LaF_3, Journal of Chemical Physics 90 (7) (1989) 3443–3457.

[5] L. Yigang, M.A. Rui, Photoluminescence from a Tb-doped photonic crystal microcavity for white light generation, Journal of Physics D: Applied Physics 43 (45) (2010) 455101.

[6] G.S.R. Raju, Y.H. Ko, E. Pavitra, J.S. Yu, J.Y. Park, H.C. Jung, B.K. Moon, Formation of $Ca_2Gd_8(SiO_4)_6O_2$ nanorod bundles based on crystal splitting by mixed solvothermal and hydrothermal reaction methods, Crystal Growth and Design 12 (2) (2011) 960–969.

[7] S. Shionoya, W.M. Yen, T. Hase, in: Phosphor Handbook, CRC press, 2007.

[8] J. Zhang, Y. Wang, L. Guo, Y. Huang, Vacuum ultraviolet–ultraviolet, X-ray, and near-infrared excited luminescence properties of SrR_2O_4:RE^{3+} (R=Y and Gd; RE=Tb, Eu, Yb, Tm, Er, and Ho), Journal of the American Ceramic Society 95 (1) (2012) 243–249.

[9] J.S. Kim, P.E. Jeon, Y.H. Park, J.C. Choi, H.L. Park, G.C. Kim, T.W. Kim, White-light generation through ultraviolet-emitting diode and white-emitting phosphor, Applied Physics Letters 85 (17) (2004) 3696–3698.

[10] X. Zhang, H.J. Seo, Color tunable and thermally stable luminescence of Tb^{3+} doped $Li_4SrCa(SiO_4)_2$ phosphors, Materials Research Bulletin 47 (8) (2012) 2012–2015.

[11] Y.-C. Li, Y.-H. Chang, Y.-S. Chang, Y.-J. Lin, C.-H. Laing, Luminescence and energy transfer properties of Gd^{3+} and Tb^{3+} in

$LaAlGe_2O_7$, Journal of Physical Chemistry C 111 (28) (2007) 10682–10688.

[12] W. Lu, Z. Hao, X. Zhang, Y. Luo, X. Wang, J. Zhang, Tunable full-color emitting $BaMg_2Al_6Si_9O_{30}:Eu^{2+}$, Tb^{3+}, Mn^{2+} phosphors based on energy transfer, Inorganic Chemistry 50 (16) (2011) 7846–7851.

[13] H.-S. Roh, I.-S. Cho, J.-S. An, C.M. Cho, T.H. Noh, D.K. Yim, D.-W. Kim, K.S. Hong, Enhanced photoluminescence property of Dy^{3+} co-doped $BaAl_2O_4:Eu^{2+}$ green phosphors, Ceramics International 38 (1) (2012) 443–447.

[14] S. Yang, W. Que, J. Chen, W.G. Liu, Nd:YAG nano-crystalline powders derived by combining co-precipitation method with citric acid treatment, Ceramics International 38 (4) (2012) 3185–3189.

[15] Y. Xu, D. Chen, Combustion synthesis and photoluminescence of $Sr_2MgSi_2O_7$:Eu,Dy long lasting phosphor nanoparticles, Ceramics International 34 (8) (2008) 2117–2120.

[16] S.H. Lee, H. Young, Y.C. Koo, Kang, Characteristics of α′- and β-$Sr_2SiO_4:Eu^{2+}$ phosphor powders prepared by spray pyrolysis, Ceramics International 36 (4) (2010) 1233–1238.

[17] V.R. Bandi, B.K. Grandhe, K. Jang, H.-S. Lee, S.-S. Yi, J.-H. Jeong, Citric based sol–gel synthesis and photoluminescence properties of un-doped and Sm^{3+} doped $Ca_3Y_2Si_3O_{12}$ phosphors, Ceramics International 37 (6) (2011) 2001–2005.

[18] R.P. Rao, Preparation and characterization of fine-grain yttrium-based phosphors by sol–gel process, Journal of the Electrochemical Society 143 (1) (1996) 189–197.

[19] Jurn W. P. Schmelzer, in: Nucleation Theory and Applications, Wiley-VCH Verlag GmbH & Co. KGaA, 2005, pp. i–xvii.

[20] W.T. Carnall, P.R. Fields, K. Rajnak, Electronic energy levels of the trivalent lanthanide Aquo Ions. III. Tb^{3+}, Journal of Chemical Physics 49 (10) (1968) 4447–4449.

[21] S.-A. Yan, Y.-S. Chang, J.-W. Wang, W.-S. Hwang, Y.-H. Chang, Synthesis and luminescence properties of color-tunable $Ba_{1-y}Sr_y$ $La_{4-x}Tb_x(WO_4)_7$ (x=0.02–1.2, y=0–0.4) phosphors, Materials Research Bulletin 46 (8) (2011) 1231–1236.

[22] H. Huang, B. Yan, Luminescence of nanophoshors Lu_2SiO_5 doped with different concentration of Tb^{3+} by in situ composition of hybrid precursors, Materials Science and Engineering, B: Advanced Functional Solid-State Materials 117 (3) (2005) 261–264.

[23] G.S. Ofelt, Intensities of crystal spectra of rare-earth ions, Journal of Chemical Physics 37 (3) (1962) 511–520.

[24] B.R. Judd, Optical absorption intensities of rare-earth ions, Phys. Rev. 127 (3) (1962) 750.

[25] J.M. Sun, W. Skorupa, T. Dekorsy, M. Helm, L. Rebohle, T. Gebel, Bright green electroluminescence from Tb^{3+} in silicon metal-oxide-semiconductor devices, Journal of Applied Physics 97 (12) (2005) 123513–123517.

[26] H.X. Zhang, C.H. Kam, Y. Zhou, X.Q. Han, S. Buddhudu, Y.L. Lam, C.Y. Chan, Deposition and photoluminescence of sol–gel derived Tb^{3+}:Zn_2SiO_4 films on SiO_2/Si, Thin Solid Films 370 (1–2) (2000) 50–53.

[27] A.D. Pearson, G.E. Peterson, W.R. Northover, Tb[sup 3+] fluorescence and nonradiative energy transfer from Gd^{3+} to Tb^{3+} in borate glass, Journal of Applied Physics 37 (2) (1966) 729–734.

[28] J.H. Ryu, Y.-G. Park, H.S. Won, S.H. Kim, H. Suzuki, J.M. Lee, C. Yoon, M. Nazarov, D.Y. Noh, B. Tsukerblat, Luminescent properties of Ca-a-SiAlON:Eu^{2+} phosphors synthesized by gas-pressured sintering, Journal of the Electrochemical Society 155 (4) (2008) J99–J104.

[29] R. Zhu, Y. Huang, H.J. Seo, The luminescence properties of Eu^{3+}-Doped borotungstate $Gd_4B_2WO_{12}$ phosphors, Journal of the American Ceramic Society 94 (10) (2011) 3380–3385.

[30] M. Arik, C. Becker, S. Weaver, J. Petroski, Thermal management of LEDs: package to system, Proceedings of SPIE 5187 (2004) 65.

[31] G.S.R. Raju, H.C. Jung, J.Y. Park, B.K. Moon, R. Balakrishnaiah, J.H. Jeong, J.H. Kim, The influence of sintering temperature on the photoluminescence properties of oxyapatite Eu^{3+}:$Ca_2Gd_8Si_6O_{26}$ nanophosphors, Sensors and Actuators, B: Chemical 146 (1) (2010) 395–402.

[32] K. Shioi, N. Hirosaki, R.-J. Xie, T. Takeda, Y. Li, Photoluminescence and thermal stability of yellow-emitting Sr-α-SiAlON:Eu²⁺ phosphor, Journal of Materials Science 45 (12) (2010) 3198–3203.

[33] K.H. Kwon, W.B. Im, H.S. Jang, H.S. Yoo, D.Y. Jeon, Luminescence properties and energy transfer of site-sensitive $Ca_{6-x-y}Mg_{x-z}$ $(PO_4)_4:Eu_y^{2+},Mn_z^{2+}$ phosphors and their application to near-UV LED-based white LEDs, Inorganic Chemistry 48 (24) (2009) 11525–11532.

[34] S. Zhang, Y. Nakai, T. Tsuboi, Y. Huang, H.J. Seo, Luminescence and microstructural features of Eu-activated $LiBaPO_4$ phosphor, Chemistry of Materials 23 (5) (2011) 1216–1224.

[35] V. Kumar, V. Mishra, S.S. Pitale, I.M. Nagpure, E. Coetsee, O.M. Ntwaeaborwa, J.J. Terblans, H.C. Swart, Surface chemical reactions during electron beam irradiation of nanocrystalline CaS:Ce [sup 3+] phosphor, Journal of Applied Physics 107 (12) (2010) 123533–123536.

[36] G. Li, Z. Hou, C. Peng, W. Wang, Z. Cheng, C. Li, H. Lian, J. Lin, Electrospinning derived one-dimensional LaOCl: Ln^{3+} (Ln=Eu/Sm, Tb, Tm) nanofibers, nanotubes and microbelts with multicolor-tunable emission properties, Advanced Functional Materials 20 (20) (2010) 3446–3456.

[37] C.-H. Chang, B.-S. Chiou, K.-S. Chen, C.-C. Ho, J.-C. Ho, The effect of In_2O_3 conductive coating on the luminescence and zeta potential of ZnS:Cu, Al phosphors, Ceramics International l 31 (5) (2005) 635–640.

[38] H.X. Zhang, S. Buddhudu, C.H. Kam, Y. Zhou, Y.L. Lam, K.S. Wong, B.S. Ooi, S.L. Ng, W.X. Que, Luminescence of Eu^{3+} and Tb^{3+} doped Zn_2SiO_4 nanometer powder phosphors, Materials Chemistry and Physics 68 (1–3) (2001) 31–35.